



OPEN ACCESS

EDITED BY

Elizabeth Arkhangelsky,
Nazarbayev University, Kazakhstan

REVIEWED BY

Rizwan Ahmad,
Pak-Austria Fachhochschule Institute of
Applied Sciences and Technology, Pakistan
Xiaobin Yang,
Harbin Institute of Technology, China

*CORRESPONDENCE

Albert Mihranyan,
✉ albert.mihranyan@angstrom.uu.se
Joey Lau,
✉ joey.lau@mcb.uu.se

†PRESENT ADDRESSES

Jules Blanc, École Normale Supérieure de Lyon,
Université Claude Bernard Lyon 1, Université de
Lyon, Villeurbanne, France
Levon Manukyan, Cytiva, Uppsala, Sweden

RECEIVED 14 November 2023

ACCEPTED 22 January 2024

PUBLISHED 05 February 2024

CITATION

Thorngren J, Vasylovskaya S, Blanc J, Wu L,
Manukyan L, Mihranyan A and Lau J (2024),
Differentiation of human pluripotent stem cells
into insulin-producing islet-like clusters using
nanofiltered cell culture medium.
Front. Membr. Sci. Technol. 3:1338366.
doi: 10.3389/frmst.2024.1338366

COPYRIGHT

© 2024 Thorngren, Vasylovskaya, Blanc, Wu,
Manukyan, Mihranyan and Lau. This is an open-
access article distributed under the terms of the
[Creative Commons Attribution License \(CC BY\)](https://creativecommons.org/licenses/by/4.0/).
The use, distribution or reproduction in other
forums is permitted, provided the original
author(s) and the copyright owner(s) are
credited and that the original publication in this
journal is cited, in accordance with accepted
academic practice. No use, distribution or
reproduction is permitted which does not
comply with these terms.

Differentiation of human pluripotent stem cells into insulin-producing islet-like clusters using nanofiltered cell culture medium

Julia Thorngren¹, Svitlana Vasylovskaya¹, Jules Blanc^{1,2†}, Lulu Wu²,
Levon Manukyan^{2†}, Albert Mihranyan^{2*} and Joey Lau^{1*}

¹Department of Medical Cell Biology, Uppsala University, Uppsala, Sweden, ²Department of Materials Science and Engineering, Uppsala University, Uppsala, Sweden

The challenge of using patient-specific, autologous stem cell therapies in clinical settings is the need for advanced cell processing and expansion technologies. These include decentralized, small-scale manufacturing at the point of care in hospitals. The highest risk for contamination in cell-based therapy products comes from animal- and human-derived components such as serum, blood components, and growth factors. To mitigate the risk of adventitious microorganism contamination, preventive measures like size-exclusion virus removal filtration of cell media components can be employed. This article examines the impact of nanofiltration using nanocellulose-based virus clearance filter paper on the differentiation of human pluripotent stem cells into insulin-producing pancreatic islets (SC-islets). The cells were monitored for biomarkers using flow cytometry and immunohistochemistry along the 7-stage differentiation protocol. The produced SC-islets were evaluated functionally using low and high glucose stimulation under dynamic perfusion conditions. Pluripotent stem cells grown in culture media filtered through 20 nm cut-off nanocellulose filters showed similar expression of desired biomarkers at each stage compared to the control group. At the end of stage 7, SC-islets exhibited a rounded shape and strong expression of insulin, glucagon, and somatostatin in both the control and filtered media groups. The present study demonstrates that SC-islets differentiated with nanofiltered media were functional.

KEYWORDS

nanofiltration, virus clearance, nanocellulose filter, stem cell-derived islets, SC-islets, cell therapy, type 1 diabetes

Introduction

Patient-specific autologous cell therapy is currently one of the most exciting avenues for developing first-in-line therapies. During autologous stem cell therapy, the patient's cells are differentiated *ex vivo* into the desired cell lineage, expanded, and then transplanted back into the patient. One of the main hurdles to the widespread use of patient-specific, autologous stem cell therapies is the need to develop cell processing and expansion technologies, including small-scale, decentralized, point-of-care, hospital-based manufacturing.

Stem cell research based on induced pluripotent stem cells (iPSC) is one example where the principles of autologous cell therapy can be realized, e.g., for the treatment of Type 1 diabetes (T1D). T1D results from the autoimmune destruction of insulin-producing pancreatic β -cells. Although subcutaneous injections of recombinant insulin can maintain physiological levels of insulin in the blood, this strategy requires regular blood glucose monitoring, which tends to vary greatly with meal intake and daily activity. To achieve a self-regulating treatment that can respond to daily blood glucose variations, the replacement of lost β -cells and retraction of autoimmunity is necessary. Several approaches can be used to generate functional β -cells for cell-based therapies, including (i) expanding primary β -cells; (ii) trans-differentiating other mature lineages into β -cells; and (iii) generating β -cells from pluripotent precursor cells (Borowiak and Melton, 2009; Lyssiotis et al., 2011).

In order to produce β -cells from iPSCs, the latter first need to differentiate toward definitive endoderm, then toward pancreatic progenitors, followed by endocrine progenitors and finally mature β -cells. To avoid poor yield (<1% of the starting population) and inability to functionally respond to glucose stimulation (Yasunaga et al., 2005), various growth factors and modulator molecules are used during each step to regulate signaling pathways, cell differentiation and maturation (Wen et al., 2011). The differentiation of iPSCs into mature β -cells is a multi-stage, time-consuming and laborious process, and each stage of cell culture and handling increases the potential risk of microorganism contamination. Therefore, the biosafety of iPSC culture is an area that requires particular attention.

Microorganism contamination in the manufacturing of stem cells can occur through several sources, including raw materials, contaminated cell lines, operators, and processing (Mahmood and Ali, 2017; Cundell et al., 2020). Normally, to avoid the risk of microbial contamination (such as that from bacteria, yeast, and fungi) due to raw materials, the cell culture media are filtration-sterilized before use with sterilizing-grade filters of 0.2–0.22 μm nominal upper cut-off size. To further minimize the risk of *mycoplasma* contamination, the media components can be sterilized with 0.1- μm -rated filters (Barone et al., 2020). However, since the size of most viruses ranges between 18 and 200 nm, none of the above filters can ensure viral safety. Animal- and human-derived components (for example, serum, blood components, and growth factors) carry the highest risk of virus contamination for cell-based therapy products (Mahmood and Ali, 2017; Barone et al., 2020). Yet, despite the known contamination risks of using animal-derived raw materials, up to 80% of Investigational New Drug (IND) submissions to the United States Food and Drug Administration (US FDA) based on stem cell technologies have been reported to use fetal bovine serum (FBS) during manufacturing (Mendicino et al., 2014). The latest ICH Q5A(R2) guideline comprehensively addresses the virus safety of biotechnology products from cell lines of human or animal origin, although no specific reference is given to iPSCs and small-scale, decentralized, point-of-care, hospital-based manufacturing (EMA, 2022).

In order to mitigate the risk of virus contamination for point-of-use biopharmaceutical manufacturing, multi-barrier defence approaches are used, such as (i) working with low-risk starting and raw materials and using manufacturing controls; (ii) using multiple in-process controls for early detection of contamination

and lot rejection; and (iii) preventive virus clearance measures to protect the cell lines from exposure to essential albeit high-risk raw materials (Cundell et al., 2020). Thus, the research gaps in point-of-use biopharmaceutical manufacturing, specifically with regard to viral safety, lie in the need for integrated approaches involving testing, risk assessment, and prevention of contamination through physical barriers. The present article addresses the use of virus-barrier filters as a part of this integrated approach.

The use of virus-barrier filters for upstream processing of cell culture media components received increased attention from both commercial vendors (Liu et al., 2000; Mann et al., 2015; Barro et al., 2020) and academic groups (Manukyan et al., 2019; Manukyan et al., 2020). While virus filtration of cell culture media is a robust method of virus clearance, the suitable filters are prone to clogging by protein aggregates and may deplete basal media components from the medium, which could negatively affect cell differentiation. This article explores the effect of nanofiltration using nanocellulose-based virus clearance filter paper on the differentiation of human embryonic stem cells into insulin-producing islets.

Materials and methods

Cell culture and pancreatic differentiation

To test if additional filtration using nanocellulose-based filter paper affects pancreatic development *in vitro*, human embryonic stem cells (hESC) (H1 cell line, Wicell[®]) were differentiated into stem cell-derived islets (SC-islets) using a seven-stage differentiation protocol (Balboa et al., 2022). Two groups were included, i.e., one control culture, differentiated according to the standard protocol, and one filter culture with additional nanofiltration of media. H1 cells were propagated in mTeSR-Plus medium (#100-0274/100-0275, STEMCELL Technologies, Vancouver, Canada) on human recombinant Laminin 521 (LN521, BioLamina, Sundbyberg, Sweden) in CO₂ incubator at 37°C, 5% CO₂, and 100% humidity. The cells were regularly monitored for pathogens and their maintenance in an undifferentiated state by the expression of pluripotency markers.

To prepare for differentiation, cells were dissociated with 0.5 mM EDTA for 10 min at 37°C and seeded on Laminin 521 coated plates at a density of 16 million cells/10 cm dish or two million cells/3.5 cm dish in mTeSR-Plus medium with the addition of 10 μM ROCK inhibitor Y-27632 (72304, STEMCELL Technologies). Differentiation started 24 or 48 h after seeding, depending on the cell density. TrypLE (Gibco, Life Technologies Corp., Grand Island, NY, United States, #12563-029) was used to make a single-cell suspension on stage 4:3 to seed cells in AggreWellsTM400 (STEMCELL Technologies) for uniform cluster formation. At the beginning of stage 6, the islet-like clusters were transferred into ultra-low attachment 6-well plates (Corning Incorporation, NY, United States) and cultured during the rest of the differentiation in suspension on a rotating platform at 95 rpm. Media compositions for every stage of the differentiation are listed in Table 1.

Basal media (500 mL) were first sterilised by filtration through a 0.22- μm filter system (PES, Corning). For the filter culture, additional media filtrations were applied using 20 nm cut-off nanocellulose-

TABLE 1 Overview of additional media components at each differentiation stage.

Monolayer				Suspension		
Definitive endoderm	Primitive gut tube	Posterior oregut	Pancreatic progenitors	Endocrine progenitors	Immature SC-islets	Mature SC-islets
Stage 1 (3 d)	Stage 2 (3 d)	Stage 3 (2 d)	Stage 4 (4 d)	Stage 5 (4 d)	Stage 6 (8 d)	Stage 7 (up to 41 d)
Activin A	Vitamin C	Vitamin C	Vitamin C	RA	LDN	T3
CHIR	FGF7	FGF7	Activin A	SANT1	GC1	NAC
		SANT1	TPB	LDN	GSiXX	ZM
		RA	RA	GC1	Alk5iII	
		LDN	FGF7	GSiXX		
		TPB	Nicotinamide	Alk5iII		
			EGF	BTC		
			LDN			
			SANT1			
ROCKi						

Abbreviations: CHIR, CHIR-99021; FGF7, Fibroblast Growth Factor 7; SANT1, (4-Benzyl-piperazin-1-yl)-(3,5-dimethyl-1H-pyrazol-4-ylmethylene)-amine; RA, retinoic acid; LDN, LDN-193189; TPB, α -Amyloid Precursor Protein Modulator; EGF, Epidermal growth factor; ROCKi (Y-27632), RHO/ROCK pathway inhibitor; GC1, thymomimetic Sobetirome; GSiXX, γ -Secretase Inhibitor XX, CAS 209984-56-5; Alk5iII, RepSox (E-616452); BTC, Betacellulin; T3 (Triiodothyronine), 3,3',5-Triiodo-L-thyronine sodium salt; NAC, N-Acetyl-L-cysteine; ZM (ZM, 447439), selective and ATP-competitive inhibitor for Aurora A and Aurora B.

based filter papers (33 μ m in thickness), including the filtration of small-molecule components and growth factors (Figure 1). The flow rate through the nanocellulose-based filters was $\sim 23.0 \text{ L m}^{-2} \text{ h}^{-1} \text{ bar}^{-1}$ for water and $\sim 18.5 \text{ L m}^{-2} \text{ h}^{-1} \text{ bar}^{-1}$ for media containing BSA. No fouling was observed under the experimental conditions, and the flow rate was stable throughout the entire experiment at 120 L/m^2 load volume. For the control culture, the standard filtered media was used after adding small molecule components and growth factors. The medium was changed every day during S1-S5 and every second day during S6 and S7.

The manufacturing of the 20 nm cut-off nanocellulose based filter paper (33 μ m in thickness) was done as reported earlier (Wu et al., 2019; Manukyan et al., 2020). The particle rejection capacity of the nanocellulose based filter paper was verified using model tracer particles, such as 20 nm Au NPs and IgG protein with dynamic light scattering (DLS) and UV-vis spectroscopy (Gustafsson et al., 2018; Wu et al., 2019). The viral clearance capacity of the filter was verified using Φ X174 small-size (28 nm) phage model as reported earlier (Manukyan et al., 2019; Wu et al., 2019).

Briefly, 0.2 wt% Cladophora nanocellulose dispersion was drained over supporting membrane to form a wet cake, which was then dried at 80°C in a hot press to produce 33 μ m-thick paper sheets. An Advantec KST filter holder (Japan) was used to mount the nanocellulose-based filter paper. The diameter of the filter paper used was 47 mm, corresponding to a 17.4 cm^2 surface area. The filtrations were done at 3 bar overhead pressure.

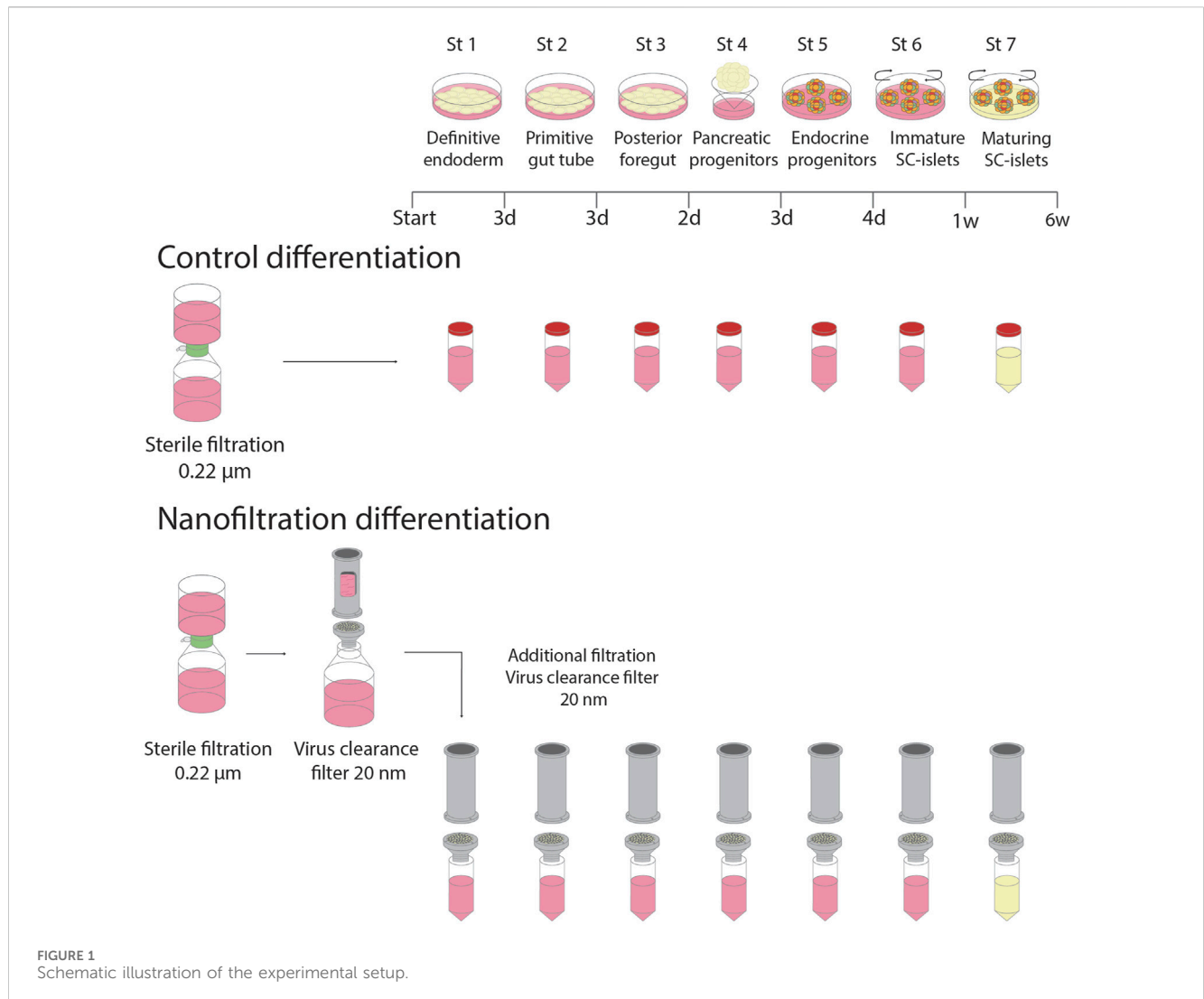
Dynamic perfusion

At the end of stage seven, 50 SC-islets were collected for perfusion and loaded into filter-covered perfusion chambers

(Suprafusion 1000, 6 channel system, Brandel, Gaithersburg, MD, United States). The SC-islets were perfused (200 μ L/min) in KRBH with the addition of 2 mg/mL bovine serum albumin (BSA) and stepwise increasing glucose concentrations. The SC-islets were first perfused in 2.8 mM glucose for 30 min. Thereafter, perfusion was performed with 16.7 mM glucose for 32 min followed by 16.7 mM glucose with the addition of exendin-4 (final concentration 10 mM) for 20 min and then again with 2.8 mM glucose for 16 min. Finally, the SC-islets were perfused with 2.8 mM glucose and KCl (final concentration 30 mM) for 24 min. Samples were collected every fourth minute during the perfusion and stored at -20°C for Insulin ELISA measurements. The results were presented as fold change, where a mean of the insulin levels secreted at low glucose exposure (2.8 mM) was calculated and divided with each sample.

Static insulin secretion

Static insulin secretion was performed at the end of the final stage of the differentiation. Glucose stimulated insulin secretion test (GSIS) was performed in triplicates of ten SC-islets from each group. Following acclimatisation at 3.3 mM glucose in KRBH with the addition of 2 mg/mL BSA during 90 min, the SC-islets were first incubated in low glucose (3.3 mM), followed by high glucose (16.8 mM) and finally low glucose with the addition of KCl (final concentration 30 mM) during 30 min, respectively. At the end of each incubation, supernatants were collected for the measurements of insulin. After the static insulin secretion assay, SC-islets were collected and sonicated once for 10 s. 50 μ L of sonicate was mixed with 125 μ L of 95% acidic ethanol to extract insulin for insulin content measurements, and the remaining sonicate was saved for DNA measurements.



ELISA measurements of insulin

The level of human insulin was measured from cell supernatants using an Ultrasensitive ELISA kit (Merckodia, Uppsala, Sweden) according to the manufacturer’s instructions.

Immunohistochemistry and image analysis

Cells on coverslips or differentiated SC-islets were fixed with 4% paraformaldehyde in PBS, washed with PBS and blocked for 1 h at room temperature in 1xPBS with 0.3% Triton X-100 (VWR, Sigma, St Louise, MO, United States) and 3% donkey serum (Jackson ImmunoResearch Laboratory, West Grove, PA, United States). Cells/SC-islets were incubated with primary antibodies overnight at 4°C, washed and incubated with secondary antibodies for 1 h at RT with subsequent washing and mounting on slides. Details of antibodies and dilutions used are stated in Table 2. Nuclei were stained with Hoechst (1:10,000; Thermo Fisher Scientific). Coverslips were mounted with Fluorescence Mounting Medium (Dako, North America Inc., Santa Clara, CA, United States).

Images were taken on a confocal microscope Zeiss LSM 780 (Carl Zeiss Microscopy GmbH, Jena, Germany).

Flow cytometry analysis

Cells/SC-islets were prepared for flow cytometry during the first day of S2 and day 39–41 of S7. Cells/SC-islets were dissociated into single-cell suspension with TrypLE (Gibco) for 5–10 min at 37°C and resuspended in 5% FBS- containing PBS. For surface marker staining with CXCR4 during S2, cells were incubated with primary antibody CXCR4/CD184 for 45 min to 1 h at room temperature prior to sample collections. For intracellular marker staining on S7, SC-islets were fixed and permeabilized using eBioscience’s fixation/permeabilization kit (dilution 1:3, eBioscience, Carlsbad, CA, United States, 00-5123-43, 00-5223-56) for 20 min. Primary antibodies were incubated overnight at 4°C in permeabilization buffer (dilution 1:10, eBioscience, 00-8833) containing 4% FBS.

After incubation, cells/SC-islets were washed twice in Permeabilization buffer and resuspended in 5% FBS- containing

TABLE 2 Antibodies used for immunohistochemistry staining and monitoring differentiation by flow cytometry.

Epitope	Origin animal	Dilution	Supplier	Assay
Primary antibody				
Insulin	Polyclonal guinea pig	1:1000	Fitzgerald, Acton, MA, United States	IHC
Glucagon	Mouse monoclonal, Alexa Fluor 488-conjugated	1:150	Invitrogen, Life Technologies Corp. Carlsstedt, CA, United States	IHC
Somatostatin	Polyclonal rabbit	1:400	Dako North America Inc., Carpinteria, CA, United States	IHC
CXCR4 (CD184)	Mouse monoclonal, PE-conjugated	1:10	BD Biosciences, United States	FC
SOX17	Goat polyclonal	1:500	R&D, Minneapolis, MN, United States)	IHC
NKX6.1	Mouse monoclonal	1:50	DSHB, Hagedorn Research Institute, Copenhagen, Denmark (DSHB Hybridoma Product F55A10, by Madsen, O.D.)	IHC
NKX6.1	Mouse monoclonal, Alexa Fluor 647-conjugated	1:80	BD Biosciences, United States	FC
NKX6.1	Mouse monoclonal, PE-conjugated	1:80	BD Biosciences, United States	FC
PDX1	Rabbit polyclonal	1:1000	Abcam, Cambridge, MA, United States	IHC
PDX1	Mouse monoclonal, PE-conjugated	1:80	BD Biosciences, United States	FC
C-peptide	Mouse monoclonal, Alexa Fluor 647-conjugated	1:80	BD Biosciences, United States	FC
IgG2a κ isotype control	Mouse monoclonal, PE-conjugated	1:80	BD Biosciences, United States	FC
IgG1 κ isotype control	Mouse monoclonal, PE-conjugated	1:80	BD Biosciences, United States	FC
IgG1 κ isotype control	Mouse monoclonal, Alexa Fluor 647-conjugated	1:80	BD Biosciences, United States	FC
Secondary antibody				
Alexa Fluor 647-conjugated	Donkey anti-guinea pig	1:300	Jackson ImmunoResearch Laboratories, West Grove, PA, United States	IHC
Cy3-conjugated	Donkey anti-rabbit	1:300	Jackson ImmunoResearch Laboratories, West Grove, PA, United States	IHC
Alexa Fluor 488-conjugated	Donkey anti-goat	1:300	Jackson ImmunoResearch Laboratories, West Grove, PA, United States	IHC
Alexa Fluor 488-conjugated	Donkey anti-rabbit	1:300	Jackson ImmunoResearch Laboratories, West Grove, PA, United States	IHC
Alexa Fluor 594-conjugated	Donkey anti-mouse	1:300	Jackson ImmunoResearch Laboratories, West Grove, PA, United States	IHC

FC, flow cytometry; IHC, immunohistochemistry.

PBS. Samples were collected on FACSCalibur (BD Bioscience) or BD Accuri C6 Plus (BD Bioscience) and cells were analysed in FlowLogic 7.2.1 (FlowLogic, Invai, Victoria, Australia). Details of the used antibodies are listed in Table 2.

Statistical analysis

Graphs and calculations for flow cytometry and functional evaluation tests were performed using Prism9 (GraphPad, San Diego, CA, United States). Functional data of control SC-islets and filter SC-islets were compared using a two-tailed student's t-test for unpaired observations. For all comparisons, a p -value <0.05 was considered as statistically significant. All values are expressed as mean \pm SEM.

Results

Prior to initiating the hESC differentiation study, the tracer particle rejection and virus clearance ability of the produced nanocellulose-based filters was verified using Au NPs, IgG, and a small-size phage model (Φ X174, 27 nm). Figure 2 summarizes the results of particle rejection characterisation. In particular, it is seen in Figures 2A–D that the nanocellulose filter paper completely rejects the 20 nm Au nanoparticles, while allowing unhindered passage of 12 nm IgG protein solution, as verified by two independent methods, i.e., DLS and UV-vis spectroscopy. Figure 2E further shows the \log_{10} removal values (LRV) for Φ X174 phage clearance by 20 nm cut-off nanocellulose-based filters. LRV >5 were observed for load volumes up to 115 L m⁻² in a duplicate run.

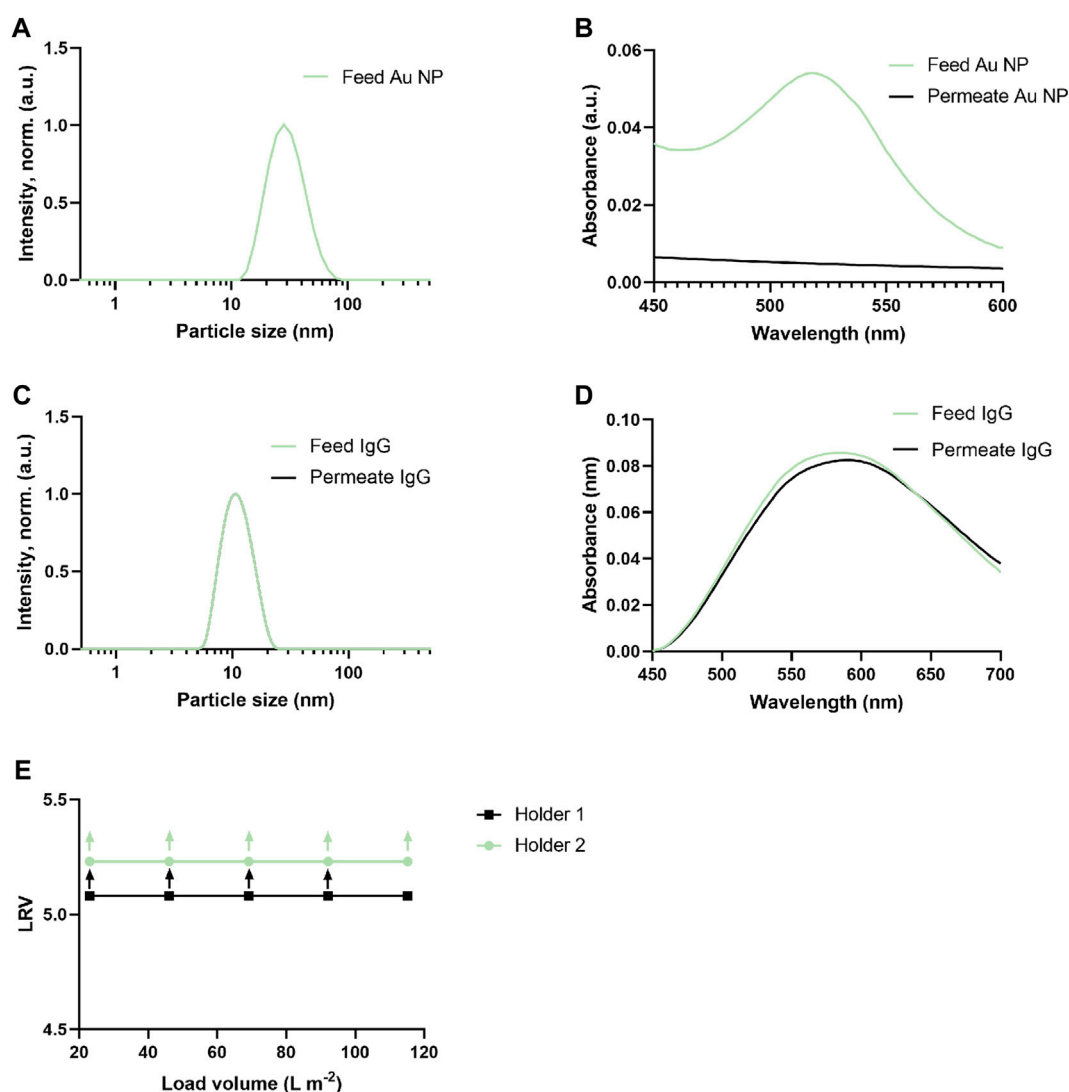


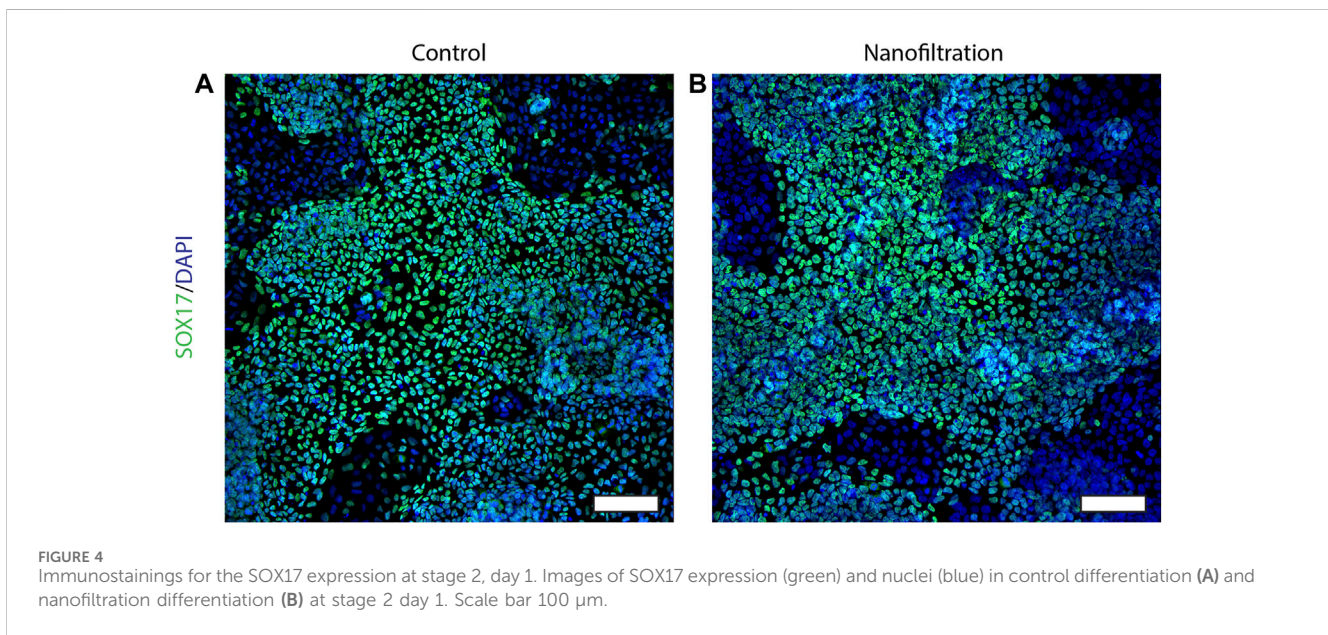
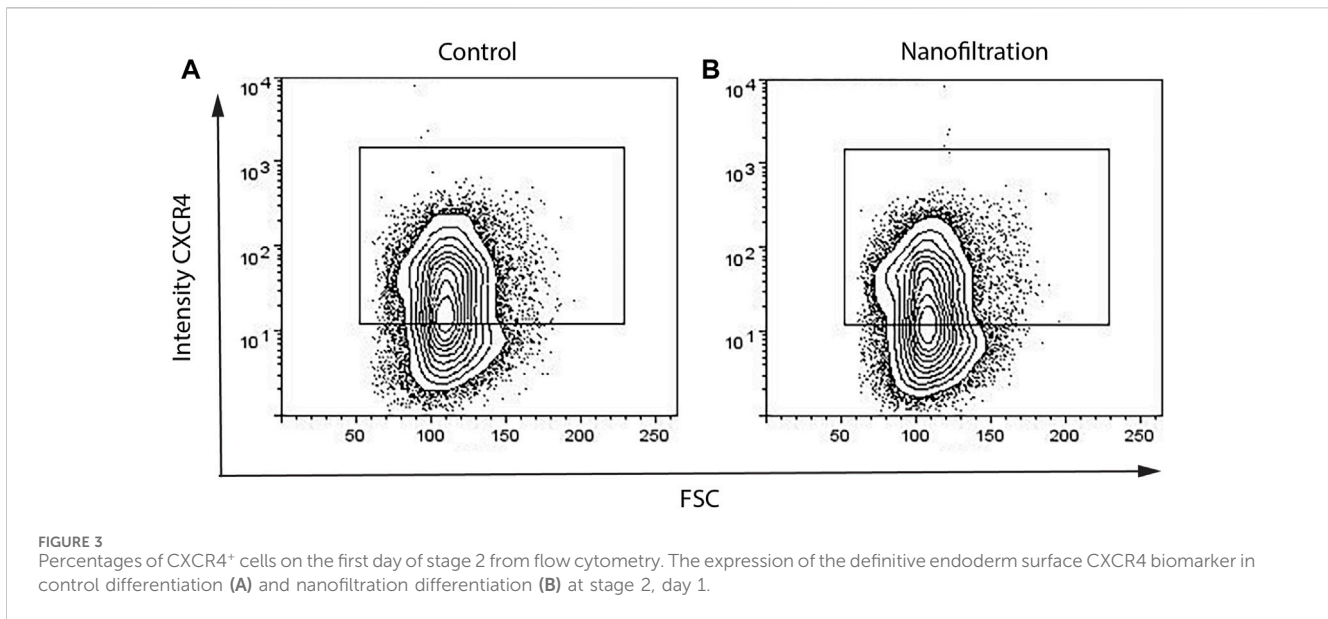
FIGURE 2

Tracer particle and virus clearance ability of nanocellulose-based filters. (A) Au nanoparticles size (intensity, normalized) distribution (feed, green curve). Permeate curve for Au nanoparticles not shown due to particle clearance and absence of measurable signal. (B) Light absorption spectra of Au nanoparticles solution filtration before (feed, green curve) and after filtration (permeate black curve), showing the removal capacity of nanocellulose filters. (C) IgG particles size (intensity, normalized) distribution before (feed, green curve) and after filtration (permeate, black curve). (D) Light absorption spectra of IgG solution before (feed, green curve) and after filtration (permeate, black curve) showing the unhindered passage of IgG through filter. (E) LRV for Φ X174 phage (27 nm) in PBS ($n = 2$). The upward arrow shows that no plaque-forming units (PFU) were detected in permeate. All the filtrations were run with a nanocellulose filters of 33 μ m of thickness at 3 bar.

Differentiation biomarker expression

The expression of CXCR4 (marker for definitive endoderm) was observed at a comparable level in both control (85.29% \pm 10.42%, $n = 3$) and filter cultures (80.16% \pm 11.87%, $n = 3$) at S2:1 of differentiation (Figures 3A, B). Moreover, to further affirm that the cells were induced towards definitive endoderm, immunohistochemical staining of SOX17 expression was performed. The SOX17 transcription factor was detected in both cultures, and the expression level between the groups was comparable (Figure 4). After 11 days of differentiation, i.e., on the third day of stage 4 (S4:2-4:3), a similar expression pattern of the multipotent pancreatic progenitor's markers PDX1 and NKX6.1 was observed in both cultures confirmed by immunohistochemical staining (Figure 5).

At the end of stage seven, i.e., the 41th day of stage 7 (S7:41), the SC-islets presented a characteristic rounded shape and the expression for insulin, glucagon and somatostatin was strong in both control SC-islets as well as in SC-islets from nanofiltration differentiation (Figure 6). To further confirm the generation of insulin-producing SC-islets, the expression of double-positive cells for beta-cell markers was confirmed with flow cytometry. The percentage of double-positive cells for transcription markers PDX1 and NKX6.1 was similar in control SC-islets (43%, $n = 1$) and filter SC-islets (30.78% \pm 11.65%, $n = 2$) (Figures 7A, B). Moreover, the expression of double-positive cells for C-peptide and NKX6.1 had a similar tendency also in both control (28.33%, $n = 1$) and filter SC-islets (23.35% \pm 4.52%, $n = 2$) during S7:25 (Figures 7C, D).



Functional evaluation

The functional insulin secretion of generated SC-islets was investigated in a dynamic (perfusion) and a static (GSIS) insulin release model at the end of differentiation (S7:36-41). Dynamic perfusion insulin release demonstrated that the insulin response of both control SC-islets and filter SC-islets was low when stimulated with high glucose (16.7 mM), only after the addition of exendin-4 the insulin response from the SC-islets increased. Exendin-4 is a peptide agonist of glucagon-like peptide (GLP-1) receptor that promotes insulin secretion. It was further observed that the insulin release of the filter SC-islets was delayed during high glucose exposure compared to the control SC-islets. When stimulated with high glucose with the addition of exendin-4, the

insulin secretion was slightly higher in the control SC-islets compared to the filter SC-islets, where the insulin release was delayed in comparison to control (Figure 8A). Following exposure to low glucose, both control SC-islets and filter SC-islets returned to basal insulin secretion. Control SC-islets secreted higher concentration of insulin compared to the filter SC-islets when the cells were depolarized by KCl. Moreover, static insulin release showed basal secretion of insulin at low glucose, increased insulin secretion at high glucose and further insulin secretion when exposed to KCl in both control and filter SC-islets (data not shown). There was no significant difference in the stimulation index from static insulin release between the control SC-islets and nanofiltered SC-islets (Figure 8B). It should finally be noted that the control SC-islets released insulin at a higher

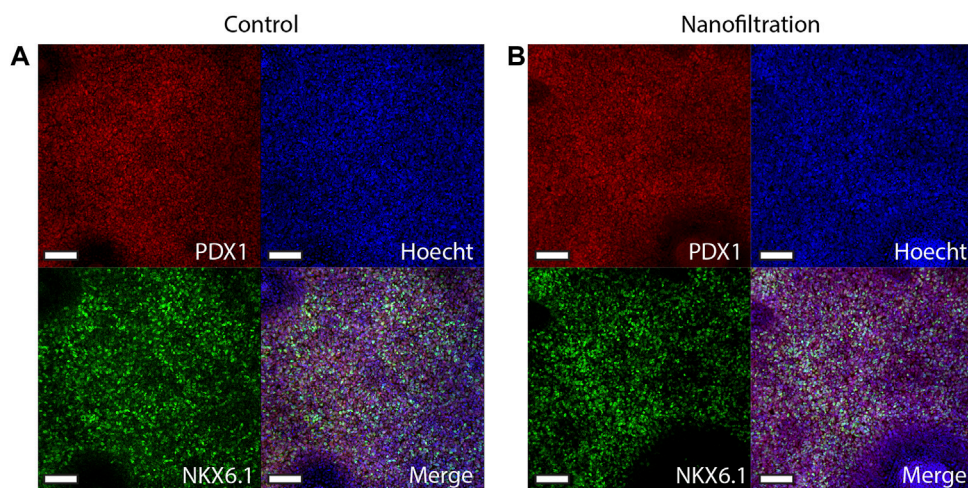


FIGURE 5 Immunostainings for the multipotent pancreatic progenitor’s markers PDX1 and NKX6.1 at stage 4, day 3 of differentiation. Images of control differentiation (A) and nanofiltration differentiation (B) for PDX1 (red), NKX6.1 (green), and nuclei (blue) at stage 4 day 3. Scale bar 100 μm .

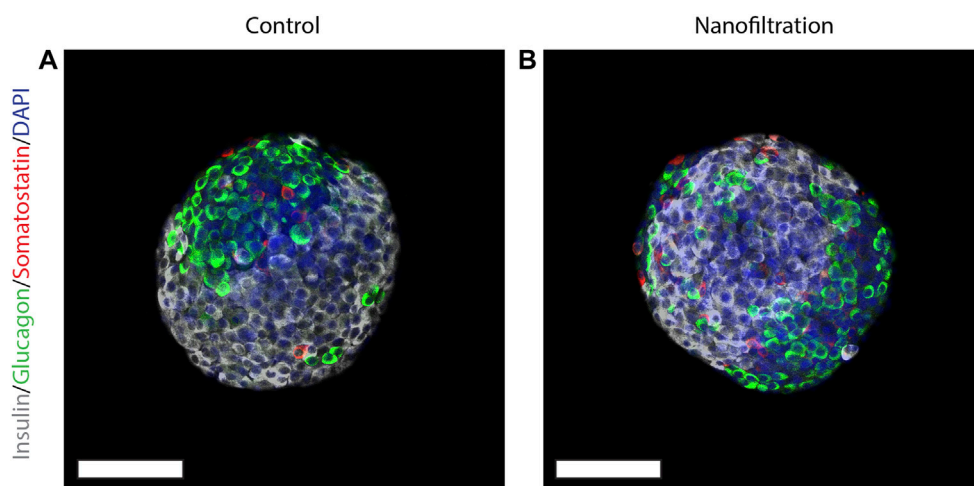


FIGURE 6 Expression of insulin, somatostatin and glucagon at final stage seven. Immunostainings for insulin (grey), somatostatin (red), glucagon (green) and nuclei (blue) in stem cell-derived islets at the final stage seven from control differentiation (A) and nanofiltration differentiation (B). Scale bar 100 μm .

concentration compared to the filter SC-islets when cells were depolarized by KCl. The delay in insulin release response and the low level of secreted insulin when exposed to solely high glucose concentration without exendin-4 for filtered sample will be discussed in the following section and could be related to the maturation of SC-islets.

Discussion

The virus clearance ability of the produced nanocellulose-based filters was verified using a small-size phage model (ΦX174 , 27 nm) before applying the filters for the differentiation of human pluripotent stem cells into insulin-producing islets. The 20 nm cut-off

nanocellulose-based filters demonstrated $\text{LRV} > 5$ for load volumes up to 115 L m^{-2} in a duplicate run, suggesting robust small-size model virus clearance, which is concordant with previously reported data (Manukyan et al., 2019). [Supplementary Material \(Supplementary Table S1\)](#) provides further details for a small-size model virus test.

In both culture variants, similar efficiency of definitive endoderm induction on the first day of stage 2 (S2:1) of differentiation was observed based on the detection of CXCR4 and SOX17 biomarkers (D’Amour et al., 2005). SOX17 is a member of the high mobility group (HMG) transcription factors that are necessary for endoderm formation, liver development, and hepatocyte differentiation in several species (Ayatollahi et al., 2012). SOX17 has been reported as an important biomarker for definitive endoderm formation in hESCs (Jiang et al., 2007). The SOX17 transcription factor was detected in both

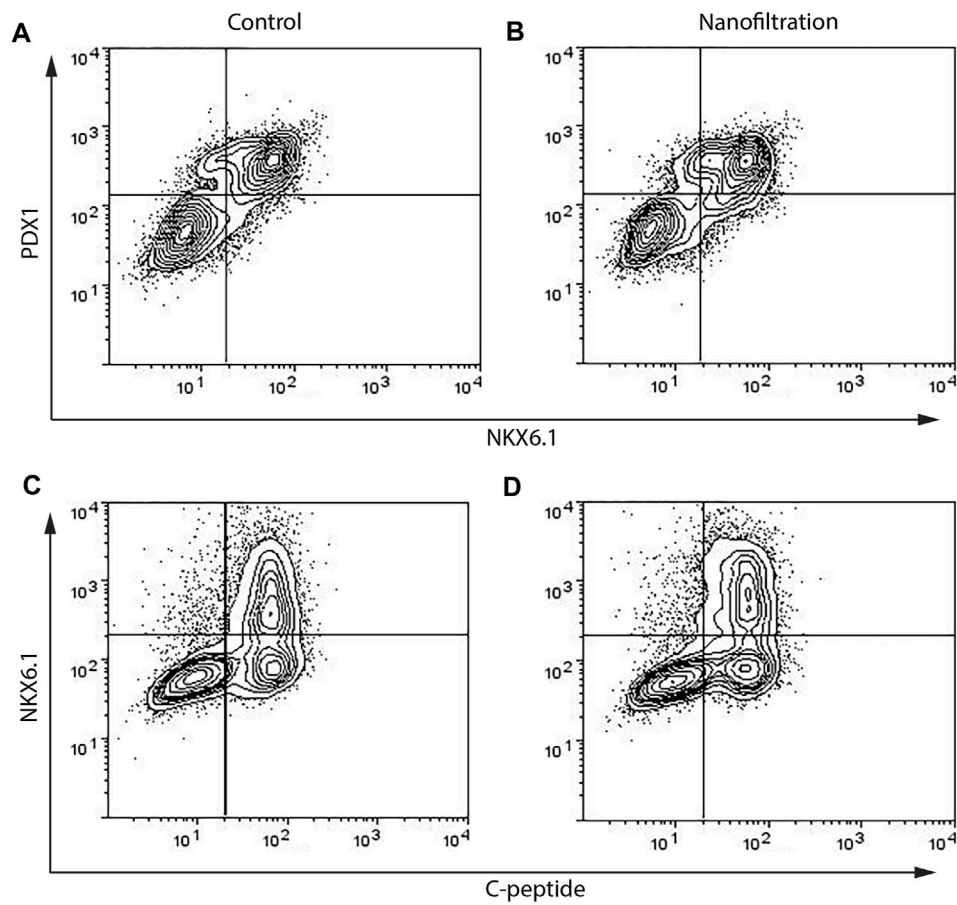


FIGURE 7 Flow cytometry data of percentages of cells double positive for PDX1 and NKX6.1 and NKX6.1 and C-peptide on final day 42 on stage 7. The expression of PDX1⁺NKX6.1⁺ and NKX6.1⁺C-peptide⁺ biomarkers in stem cell-derived islets at the final stage 7 from control differentiation (A,C) and nanofiltration differentiation (B,D).

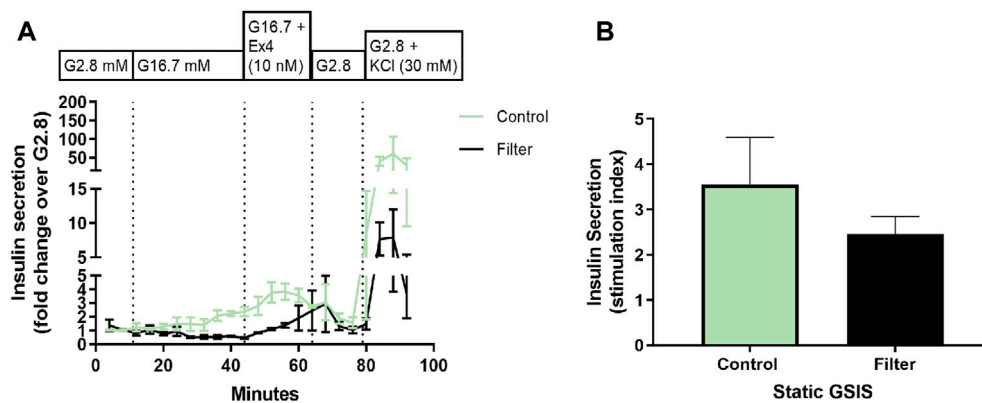


FIGURE 8 Functional evaluation of stem cell-derived islets at stage 7, day 25–38. (A) Perfusion (dynamic insulin release test) of stem cell-derived islets at the final stage 7 from control differentiation (green) and nanofiltration differentiation (black) with the following conditions: low glucose (2.8 mM), high glucose (16.7 mM), high glucose with the addition of exendin-4 (10 nM) and low glucose with the addition of KCl (30 mM). Insulin secretion is expressed as a fold change over low glucose (2.8 mM). All values are given as mean \pm SEM, $n = 2-3$. (B) Stimulation index (SI; the ratio of insulin secretion at high versus low glucose) from static insulin secretion test of stem cell-derived islets at final stage seven from control differentiation (green) and nanofiltration differentiation (black). All values are given as mean \pm SEM, $n = 3$.

cultures, and the expression level between the groups was comparable. Moreover, our results demonstrated similar expression of PDX1 and NKX6.1 in filter SC-islets compared to control SC-islets. PDX1 and NKX6.1 are expressed early during pancreatic beta cell development and are important for the functional insulin-releasing ability of beta cells (Taylor et al., 2013; Gao et al., 2014). The comparable expression of C-peptide in both control and filter SC-islets demonstrated that the cells differentiated towards beta-cells. At the end of stage seven, both control and filter SC-islets presented a characteristic rounded shape and expression for the islet hormones insulin, glucagon and somatostatin.

It can be concluded that the expression of pluripotency markers of the SC-islets was consistent in both groups during the different stages of differentiation (i.e., a 48-day long, multi-stage differentiation protocol) towards pancreatic development, and no aberrations in the expression of biomarkers were observed following the nanofiltration.

Dynamic functional evaluation of the differentiated SC-islets demonstrated low secretion of insulin when exposed to high glucose in both control and filter SC-islets. Exendin-4 was needed to promote the insulin secretion. Filter SC-islets showed a slight delay of insulin secretion when exposed to high glucose. The delay in insulin release and the lower level of secreted insulin when exposed to solely high glucose concentration without exendin-4 could be related to the maturation of SC-islets. Recent studies demonstrate similar results where SC-islets during the early stage 7 were not triggered by high glucose and did not show a normal biphasic insulin secretion pattern characteristic for adult human islets. But when the differentiation protocol was prolonged and the SC-islets were further cultured during stage 7, the SC-islets continued to mature, and insulin release was triggered by high glucose concentrations in a normal biphasic insulin secretion manner, similar to primary adult islets (Balboa et al., 2022). Further extension of culturing SC-islets resulted in higher insulin secretion than primary adult islets. Moreover, there was no significant difference in the stimulation index from static insulin release between the control SC-islets and nanofiltered SC-islets. It is important to note that the functional evaluation demonstrated that the nanofiltration of cell culture media did not affect the differentiation of hESC towards SC-islets. The insulin releasing function of SC-islets was not influenced by the nanofiltration, demonstrating that the nanofiltration did not affect the SC-islets during differentiation and at the last stage, when fully differentiated.

During the differentiation of hESC towards SC-islets, the expression of maturation markers such as CXCR4, PDX1, and NKX6.1 have been at accepted levels according to flow cytometry and in similar percentages to control differentiation. The expression of similar markers has been seen to be expressed as well with immunohistochemical staining throughout the stages of the differentiation. At the end of the final stage seven, expression of insulin, glucagon and somatostatin were expressed in both control SC-islets as well as in SC-islets cultured with nanofiltered media. Furthermore, the functional evaluations of the SC-islets at the end of the differentiation demonstrates that the ability to release insulin when stimulated by glucose was not affected by the nanofiltration of the cell culture media.

Our results indicate that media filtration using nanocellulose-based filter paper does not inhibit the differentiation of hESC into functional insulin-producing SC-islets. As novel cell-based therapies come closer to being tested in clinical trials, the present work

investigates overlooked aspects of biosafety in developing new medical treatments based on stem cells.

Conclusion

Viral safety of biotechnology products derived from cell lines of human and animal origin is critical for advancement of cell therapies. The use of virus-barrier filters for the upstream processing of cell culture media components received increased attention in recent years. While virus filtration of cell culture media is a robust method of virus clearance, the suitable filters may deplete critical media components from the feed, which could negatively affect hESC/iPSC differentiation. The present article reports for the first time the effect of nanofiltration using nanocellulose-based virus clearance filter paper on the differentiation of human PSCs into insulin-producing islets. The SC-islets express desired differentiation biomarkers at the respective stage and exhibit strong signals for insulin, glucagon and somatostatin in immunohistochemistry staining experiments. Furthermore, the results suggest that the SC-islets secrete insulin in a regulated manner.

Data availability statement

The original contributions presented in the study are included in the article/[Supplementary Material](#), further inquiries can be directed to the corresponding authors.

Ethics statement

Ethical approval was not required for the studies on humans in accordance with the local legislation and institutional requirements because only commercially available established cell lines were used.

Author contributions

JT: Data curation, Investigation, Writing—original draft. SV: Data curation, Investigation, Project administration, Writing—original draft. JB: Data curation, Investigation, Writing—review and editing. LW: Data curation, Investigation, Writing—original draft. LM: Investigation, Project administration, Writing—review and editing. AM: Conceptualization, Data curation, Funding acquisition, Methodology, Project administration, Resources, Supervision, Writing—original draft, Writing—review and editing. JL: Conceptualization, Data curation, Funding acquisition, Methodology, Project administration, Resources, Supervision, Writing—original draft, Writing—review and editing.

Funding

The author(s) declare financial support was received for the research, authorship, and/or publication of this article. The project was funded by Knut and Alice Wallenberg Foundation (Bridge grant 2018.01141), EIT Health Innovation by Idea (19104 Veripap

project), the Swedish Child Diabetes Fund, the Ernfors family foundation, as well as the national strategic research programmes Excellence of Diabetes Research in Sweden (Exodiab) and StemTherapy. LW was a recipient of a Chinese National Academy of Sciences scholarship (201708420160) for Ph.D. studies abroad.

Acknowledgments

The skilled technical assistance of Zhanchun Li and Lisbeth Ahlqvist at the Department of Medical Cell Biology, Uppsala University, are gratefully acknowledged.

Conflict of interest

One of the corresponding authors (AM) is the inventor behind IP for virus removal filter paper.

References

- Ayatollahi, M., Sanati, M., Kabir Salmani, M., and Geramizadeh, B. (2012). Differential expression pattern of the human endoderm-specific transcription factor sox17 in various tissues and cells. *Int. J. Organ Transplant. Med.* 3 (4), 183–187.
- Balboa, D., Barsby, T., Lithovius, V., Saarikäki-Vire, J., Omar-Hmeadi, M., Dyachok, O., et al. (2022). Functional, metabolic and transcriptional maturation of human pancreatic islets derived from stem cells. *Nat. Biotechnol.* 2022, 1042–1055. doi:10.1038/s41587-022-01219-z
- Barone, P. W., Wiebe, M. E., Leung, J. C., Hussein, I., Keumurian, F. J., Bouessa, J., et al. (2020). Viral contamination in biologic manufacture and implications for emerging therapies. *Nat. Biotechnol.* 38 (5), 563–572. doi:10.1038/s41587-020-0507-2
- Barro, L., Nebie, O., Chen, M.-S., Wu, Y.-W., Koh, M. B., Knutson, F., et al. (2020). Nanofiltration of growth media supplemented with human platelet lysates for pathogen-safe xeno-free expansion of mesenchymal stromal cells. *Cytotherapy* 22 (8), 458–472. doi:10.1016/j.jcyt.2020.04.099
- Borowiak, M., and Melton, D. A. (2009). How to make β cells? *Curr. Opin. Cell Biol.* 21 (6), 727–732. doi:10.1016/j.ccb.2009.08.006
- Cundell, T., Drummond, S., Ford, I., Reber, D., and Singer, D. (2020). Risk assessment approach to microbiological controls of cell therapies. *PDA J. Pharm. Sci. Technol.* 74 (2), 229–248. doi:10.5731/pdajpst.2019.010546
- D'Amour, K. A., Agulnick, A. D., Eliazar, S., Kelly, O. G., Kroon, E., and Baetge, E. E. (2005). Efficient differentiation of human embryonic stem cells to definitive endoderm. *Nat. Biotechnol.* 23 (12), 1534–1541. doi:10.1038/nbt1163
- EMA (2022). ICH Q5A(R2) Guideline on viral safety evaluation of biotechnology products derived from cell lines of human or animal origin - scientific guideline EMA/CHMP/ICH/804363/2022. <https://www.ema.europa.eu/en/ich-q5ar2-guideline-viral-safety-evaluation-biotechnology-products-derived-cell-lines-human-or-animal-origin-scientific-guideline>.
- Gao, T., McKenna, B., Li, C., Reichert, M., Nguyen, J., Singh, T., et al. (2014). Pdx1 maintains β cell identity and function by repressing an α cell program. *Cell Metab.* 19 (2), 259–271. doi:10.1016/j.cmet.2013.12.002
- Gustafsson, O., Gustafsson, S., Manukyan, L., and Mhrianyan, A. (2018). Significance of brownian motion for nanoparticle and virus capture in nanocellulose-based filter paper. *Membranes* 8 (4), 90. doi:10.3390/membranes8040090
- Jiang, W., Shi, Y., Zhao, D., Chen, S., Yong, J., Zhang, J., et al. (2007). *In vitro* derivation of functional insulin-producing cells from human embryonic stem cells. *Cell Res.* 17 (4), 333–344. doi:10.1038/cr.2007.28
- The remaining authors declare that the research was conducted in the absence of any commercial or financial relationships that could be construed as a potential conflict of interest.

Publisher's note

All claims expressed in this article are solely those of the authors and do not necessarily represent those of their affiliated organizations, or those of the publisher, the editors and the reviewers. Any product that may be evaluated in this article, or claim that may be made by its manufacturer, is not guaranteed or endorsed by the publisher.

Supplementary material

The Supplementary Material for this article can be found online at: <https://www.frontiersin.org/articles/10.3389/frmst.2024.1338366/full#supplementary-material>

Liu, S., Carroll, M., Iverson, R., Valera, C., Vennari, J., Turco, K., et al. (2000). Development and qualification of a novel virus removal filter for cell culture applications. *Biotechnol. Prog.* 16 (3), 916–934. doi:10.1021/bp000027m

Lyssiotis, C. A., Lairson, L. L., Boitano, A. E., Wurdak, H., Zhu, S., and Schultz, P. G. (2011). Chemical control of stem cell fate and developmental potential. *Angew. Chem. Int. Ed.* 50 (1), 200–242. doi:10.1002/anie.201004284

Mahmood, A., and Ali, S. (2017). Microbial and viral contamination of animal and stem cell cultures: common contaminants, detection and elimination. *J. Stem Cell Res. Ther.* 2 (5), 1–8. doi:10.15406/jsrt.2017.02.00078

Mann, K., Royce, J., Carbrelo, C., Smith, R., Zhu, R.-R., Zeng, Y., et al. (2015). Protection of bioreactor culture from virus contamination by use of a virus barrier filter. *BMC Proc.* 9, P22–P23. doi:10.1186/1753-6561-9-s9-p22

Manukyan, L., Marinaki, M.-E., and Mhrianyan, A. (2020). Would 20 nm filtered fetal bovine serum-supplemented media support growth of CHO and HEK-293 cells? *ACS Appl. Bio Mater.* 3 (12), 8344–8351. doi:10.1021/acsabm.0c01372

Manukyan, L., Padova, J., and Mhrianyan, A. (2019). Virus removal filtration of chemically defined Chinese Hamster Ovary cells medium with nanocellulose-based size exclusion filter. *Biologicals* 59, 62–67. doi:10.1016/j.biologics.2019.03.001

Mendicino, M., Bailey, A. M., Wonnacott, K., Puri, R. K., and Bauer, S. R. (2014). MSC-based product characterization for clinical trials: an FDA perspective. *Cell Stem Cell* 14 (2), 141–145. doi:10.1016/j.stem.2014.01.013

Taylor, B. L., Liu, F. F., and Sander, M. (2013). Nkx6.1 is essential for maintaining the functional state of pancreatic beta cells. *Cell Rep.* 4 (6), 1262–1275. doi:10.1016/j.celrep.2013.08.010

Wen, Y., Chen, B., and Ildstad, S. T. (2011). Stem cell-based strategies for the treatment of type 1 diabetes mellitus. *Expert Opin. Biol. Ther.* 11 (1), 41–53. doi:10.1517/14712598.2011.540235

Wu, L., Manukyan, L., Mantas, A., and Mhrianyan, A. (2019). Nanocellulose-based nanoporous filter paper for virus removal filtration of human intravenous immunoglobulin. *ACS Appl. Nano Mat.* 2 (10), 6352–6359. doi:10.1021/acsanm.9b01351

Yasunaga, M., Tada, S., Torikai-Nishikawa, S., Nakano, Y., Okada, M., Jakt, L. M., et al. (2005). Induction and monitoring of definitive and visceral endoderm differentiation of mouse ES cells. *Nat. Biotechnol.* 23 (12), 1542–1550. doi:10.1038/nbt1167

Glossary

Alk5Iii	RepSox (E-616452)
BSA	Bovine serum albumin
BTC	Betacellulin
CHIR	CHIR-99021
CXCR4	C-X-C chemokine receptor type 4
DLS	Dynamic light scattering
EGF	Epidermal growth factor
FBS	Fetal bovine serum
FGF7	Fibroblast Growth Factor 7
GC1	thromimetic Sobetirome
GSIS	Glucose stimulated insulin secretion
GSiXX	γ -Secretase Inhibitor XX - CAS 209984-56-5
hESC	human embryonic stem cells
iPSC	induced pluripotent stem cells
KRBH	Krebs-Ringer bicarbonate-HEPES buffer
LDN	LDN-193189
LRV	Log ₁₀ removal values
NAC	N-Acetyl-L-cysteine
NKX6.1	Homeobox protein Nkx-6.1
NPs	Nanoparticles
PBS	Phosphate Buffered Saline
PDX1	Pancreas/duodenum homeobox protein 1
PFU	Plaque-forming units
PSCs	Pluripotent stem cells
RA	Retinoic acid
ROCKi (Y-27632)	RHO/ROCK pathway inhibitor
SANT1	(4-Benzyl-piperazin-1-yl)-(3,5-dimethyl-1-phenyl-1H-pyrazol-4-ylmethylene)-amine
SC-islets	Stem cell-derived islets
SOX17	Transcription factor SOX-17
T1D	Type 1 diabetes
T3 (Triiodothyronine)	3,3',5'-Triiodo-L-thyronine sodium salt
TPB	α -Amyloid Precursor Protein Modulator
ZM (ZM 447439)	selective and ATP-competitive inhibitor for Aurora A and Aurora B